JOURNAL OF MATERIALS SCIENCE 24 (1989) 2262–2274

The graphite gauge and its application to the measurement of crack velocity

B. STALDER*, PH. BÉGUELIN, A. C. ROULIN-MOLONEY‡ H. H. KAUSCH
Laboratoire de Polymères, Ecole Polytechnique Fédérale de Lausanne, CH-1007 Lausanne, Switzerland

Existing methods for the measurement of crack position (and hence crack velocity) are briefly reviewed. Those methods are principally based on the optical, mechanical, electrical or acoustic behaviour of a cracking sample, or on an inspection of the fracture surfaces. None of the above techniques fulfills all conditions required to measure continually slow and fast crack growth in polymers up to 250° C, the only method capable of doing this is a potentiometric gauge without support. The development and application of such a graphite gauge to crack propagation in polymers is described in this paper. The experimental arrangement in general and the results obtained from "instrumented samples" in Charpy impact tests and from crack propagation across an interface between dissimilar materials are discussed and the advantages (large sensitivity, range of crack speeds from 10^{-7} to 10^{3} m sec^{-1}) and disadvantages (gauge is also sensitive to plastic deformations) are indicated.

1. Introduction

The techniques currently employed for the measurement of crack position and hence, crack velocity, may be divided into five groups [1, 2]: optical methods; fractography; compliance methods; electrical methods; acoustic methods. Each group will be reviewed with the objective of evaluating the advantages and disadvantages of the various methods particularly with application to the fracture testing of polymers.

1.1. Optical methods

The position of the crack tip may often be determined by direct observation of the surface of the specimen. A microscope or a magnifying glass is usually necessary to see the tip and to measure the position with sufficient accuracy. The crack speed may be estimated by extrapolation between successive values of $a(t)$, where a is the fracture length, and t the time. A measuring grid applied to the specimen (for example with a photosensitive lacquer [3]) can assist in the determination of crack position. Alternatively, a microscope with a graduated objective or a cathetometer, avoids the necessity of applying a grid to each sample. However, it is necessary to take into account the possible displacements, for example, rotation in a compact tension specimen, or flexion in a three-point bending sample. When crack speeds are greater than a few millimetres a minute, it is necessary to use some kind of external method of recording the event such as a video recorder or a high-speed camera. In certain cases special techniques (photoelasticity, Moiré fringes, shadowgraphy) can highlight the crack front. The limitations of these methods are given in Table I. The accuracy of the method depends on the maximum allowed distance between measuring points and only discrete points can be determined. Furthermore, at high crack velocities the use of an ultrahigh-speed camera is obligatory. This is cumbersome and expensive in equipment and the analysis of the results is time-consuming. An image analysis system is required for the digitilization of the data.

1.2. Fractography

Fractography gives a very important source of information on the physics of fracture. Furthermore, by the post-mortem analysis of the fracture surface precise information is obtained on the position and shape of the crack. For example, rapid changes in crack speed or crack arrest can induce changes in the fracture surface topography. If the fracture is stable between two events, it is possible to estimate the mean crack speed by comparison with the force–time diagram. Particularly favourable conditions are found in testing double torsion or double cantilever beam samples where crack propagation is steady. At constant crosshead speeds, the critical stress intensity factor, K_c, remains constant and thus also the crack speed. An example is given in Fig. 1 for the double torsion geometry where the total time for which the load remains constant is Δt, and the length fractured is Δa. From this, a precise calculation of crack speed is then possible.

Filled resins often leave no such traces on the fracture surface. In order to determine crack position at a certain stage in the test, it is possible to reduce the applied load by a small amount such that the crack

* *Present address*: Vuille SA, CH-1700 Fribourg, Switzerland.
‡ *Present address*: Tetra Pak Romont SA, Development Department, CH-1680 Romont Fr, Switzerland.

0022–2461/89 $03.00 + .12 © *1989 Chapman and Hall Ltd.*

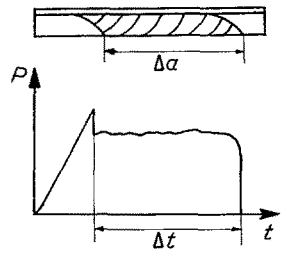

Figure 1 Fracture of a PMMA sample in double torsion. Schematic diagram of the fracture surface and the load–time diagram.

remains stationary but stays open, and then an ink of very low viscosity can be applied. Once the ink had dried the test may be re-started. The position of the crack front may be readily determined after complete fracture. Care must be exercised, however, in the choice of ink as some inks can cause stress corrosion cracking in certain polymers.

An elegant way to apply the technique of fractography is to superimpose an ultrasonic shear vibration (of frequency f_0) on to the main load. In the case of a brittle material, crack propagation is perpendicular to the principal tensile direction, therefore the crack will oscillate in a periodic manner around the main fracture plane. This method is known by the name of its inventor, Kerkhof [4], and allows the determination of crack advance during a time equivalent to $1/f_0$. Judging from recent reports [5] which describe attempts to refine this method, the approach is still of current interest. The technique is of particular use for high-speed fracture. If the ultrasonic signal is coded, then it is possible to measure not only the speed as a function of crack position, but also the position as a function of time.

1.3. Compliance methods

Specimen compliance can be related to the dimensions, the elastic modulus and to crack length. This means that by knowing the other parameters and the relationship between them it is possible to deduce the crack length. The sensitivity of this method is, however, low especially for short cracks in most common geometries. The more common technique is to measure the back face strain (BFS). A strain gauge is bonded to the back of the specimen in the plane of the crack. Deans and Richards [6] claim that this technique is more sensitive than the potential difference method which will be described in Section 1.4. This technique may be applied to all materials. By normalizing the specimen dimensions, Deans and Richards defined the function $A^*(a/W)$ which is characteristic of a certain geometry

$$A^*\left(\frac{a}{W}\right) = (\mathrm{BFS})BW\frac{E}{P}$$

This function is defined by Deans and Richards [7, 8] for the compact tension geometry. Although this is an attractive method, it is scarcely applicable to certain geometries, such as the double cantilever beam, which are too long to give the required sensitivity.

TABLE I Summary of the principal methods of measuring crack velocity

Method	Materials possible	Temperature of test	Cont. or discrete measurement	Control possible	Length measured	Range of speeds	Comments
Optical methods							
Cathetometry	All	All	Discrete	Manual	Sample surface	Slow	Measurement of speed and accuracy depends on distance between values of a
Photography	All	All	Discrete	None	Sample surface	Slow	
High speed photography	All	All	Discrete	None	Sample surface	Fast	
Fractography							
Penetrating ink	All	Ambient	1 point	Not possible	Complete profile	Inappropriate	Useful for a prior to test
Marks on fracture surface	Unfilled Brittle materials	High temp. $< 250°C$ (oscillator)	Discrete Discrete but many points	"post-mortem"	Partial/complete Complete profile if coded	Poss. with $P(t)$ Medium to Fast	Complementary method Powerful method
Forced oscillations							
Compliance							
Compliance in force axis	All	All	Discrete if plastic def. is negligible Continuous if perf. elastic.	Yes with steps	Mech. mean	Slow due to load–unload cycles	Rarely used. Low sensitivity.
Back face strain	All	$< 250°C$ (gauges)	Continuous	Yes		Slow to fast	Linear variation with K_c and quasi-linear with a, for CT
Potentiometric methods							
Potential drop	Conductors	High	Continuous	Yes	Electric mean	Slow to fast	Calibration necesssary
Eddy current	Conductors	$< 50°C$ (bobbin)	Continuous	Yes	Mean f (thickness)	Slow	Calibration unnecessary
Bonded gauges	All	$< 250°C$	Contin. if layer Discrete if grid	Yes	Surface	Slow to fast	Fracture simult. in gauge and material?
Gauge of conductive lines without support	Insulators	$< 300°C$ (lacquer)	Discrete dep. on grid geometry	Yes with steps	Surface	Slow to fast	Possible to use wide range of geometries
Acoustic methods							
By reflection or diffraction	Elastic mater. Damping by elasto-plastic or viscoelastic materials	$< 250°C$ (detectors)	Quasi-continuous	Yes	Mean area fractured	Slow to fast	Low sensitivity

Because the back face strain is approximately linearly related to K_c and crack length, this method could be used for servo-control during, for example, a fatigue test [9], the principal advantage being that the crack travels at constant speed. The measurement of da/dN (N = the number of load cycles) as a function of ΔK_c is in this case much more accurate if the maximum and minimum loads are controlled by continual variation of the parameters ΔK_c and da/dN.

1.4. Potentiometric methods

The potentiometric methods utilize the electrical conductivity of the material under test. In the case of polymeric systems these are either intrinsically conducting polymers [10] or materials filled with metallic particles [11, 12]. A current passing through the specimen induces a potential field, the distribution of which depends on the geometry. If the contact points are well chosen it is possible to deduce the crack length [13].

This technique is normally applied to metallic materials and due to their high conductivity, in general two separate circuits are used. One of these circuits supplies a regulated current to the specimen and the other allows the measurement of the resulting tension at two points close to the crack (see Fig. 2). The relationship between the difference of potential and the crack length allows either an experimental or a theoretical calibration [14, 15] which is a function of the specimen geometry and the position of the four measuring points. It is usual to employ direct current in spite of the fact that it is possible to take advantage of the alternating current, which follows the free surfaces of a conductor [16].

By this method it is also possible to identify crack fronts that are not straight providing they are close to the surface and extend a certain distance from the defect which is being characterized [17]. An example is an elliptical crack in a plate under tension, in a cylinder or a tube. The potential at a number of points around the crack must be known, this number depending on the required accuracy.

The crack length measured by these potentiometric methods is an "electrical mean". The fracture mechanisms operating in the zone at the crack tip can have a strong influence on the local resistivity; for example, plastic deformation, void formation, microcracks, structural modifications or change in crystallinity, atomic or molecular migration. This "electrical mean" does not generally coincide with the mechanical variations which define G_c. When the process zone at the crack tip is large the real crack length can be very different to that determined electrically and this can

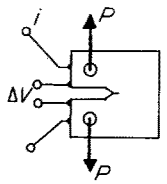

Figure 2 Compact tension sample showing the position of current supply and voltage measurement as used in the electrical measurement of crack length.

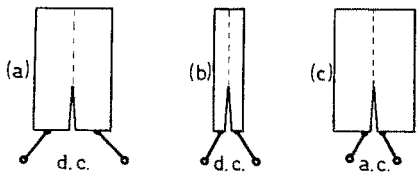

Figure 3 Three types of conductive gauges according to the type of current supply used and the shape of the conductive layer, narrow or wide.

give rise to resulting error in the estimation of K_c and G_c. In order to avoid this problem it is possible to use bonded crack gauges which are similar in conception to strain gauges [18]. However, the application of a layer of adhesive, an insulating support, such as an epoxide or polyimide, and a layer of constantan, can often cause problems in that the crack does not propagate simultaneously in the material and the constantan layer. This implies paradoxically that the properties of the material under test must be known in order to choose a suitable gauge. Direct application of a gauge by vaporization avoids the necessity of a support and the gauge is, as a result, more accurate [19].

Amongst the available gauges of this type there are three configurations as shown in Fig. 3.

(a) similar to potential drop techniques, this arrangement must be calibrated either theoretically or experimentally. Small variations in the crack trajectory do not notably change the measurements;

(b) a band of length much greater than width results in a resistance proportional to twice the crack length. Even slight changes in the crack trajectory will falsify the results;

(c) using alternating current the crack contour, s, is measured and not the component in the x-direction, a_x, which is used to calculate K_c. However, the derivative of s gives the absolute value of the speed vector, s. This technique is of interest for the study of crack arrest, branching or crack deviation especially where the crack speed can be correlated with the fracture surface topography.

In the polymer field a number of workers have used a series of conductive lines painted on to the specimen using silver ink (see Fig. 4). This technique has been used for quasistatic [20], dynamic [21] and cyclic loading [22]. However, during fracture between each discrete line no measurements can be made. This is not a serious problem if the fracture is continuous but if the fracture is unstable or occurs with rapid changes in velocity, the phenomenon cannot be measured with accuracy. This technique does, however, give a useful complement to visual methods which also rely on an estimation of the mean crack speed. The equipment required consists of a stabilized power supply and a

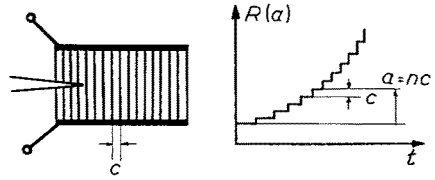

Figure 4 Crack gauge with conductive lines. Each jump in resistance corresponds to an increase, c, in the crack length.

voltmeter. The output is in the form of a number of jumps in the resistance–time curve as each successive line is broken.

1.5. Acoustic methods

An ultrasonic wave propagating in a solid is disturbed by regions where there is a change in the elastic properties. This characteristic is being exploited in the acoustic microscopes which are now becoming available [22]. A defect such as a crack which provides a discontinuity of the material gives rise to a plane of reflection of the original waves. This is recorded either by the transducer which produced the original signal, or by a separate detector. The size of the defect is deduced from the amplitude of the signal. This method has been used for some time in quality control. The same principle can be applied to fracture mechanics specimens [1]. Some improvements have been suggested which allow the diffraction produced at the crack tip to be used [24].

This method is rather difficult to apply in practice and not enough information is available for specimens other than compact tension. In spite of this, the technique is of considerable value for specific problems, such as, the study of the mechanisms of crack opening and closure [24] or the determination of very short crack length [25]. The principal characteristics of these various methods for the measurement of crack speed are summarized in Table I.

An ideal method for the measurement of crack speed in polymers would have the following characteristics: applicable to electrically insulating polymers; measurement possible up to 250° C in ambient atmosphere; continuous or quasi-continuous measurement; applicable to slow and fast crack speeds; applicable to both plane and grooved surfaces; measurement of crack lengths in the range 5 to 100 mm. It can be seen from studying Table I that the only method which has the potential for meeting all the above requirements is a potentiometric gauge without a support. The idea was first suggested in 1979 by Geury and Dieudonne [19] but was not exploited for the systematic measurement of crack velocities.

2. The graphite gauge

Taking a section of length, b, of a conductor with a cross-section Le, a homogeneous current of density j runs normal to the supposed path of the crack. The electrical resistance is given by

$$R_0 = \frac{\varrho b}{eL} \tag{1}$$

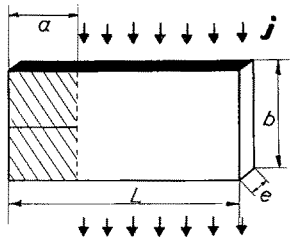

Figure 5 Electric model of a crack gauge in the form of a continuous layer: the conductor, of area $b(L - a)$, is crossed by a homogeneous current of density j.

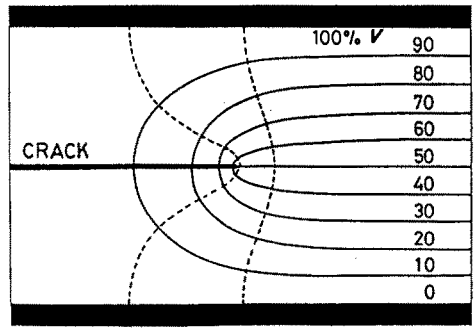

Figure 6 Experimental determination of the lines of current in (– – –) the gauge and (——) the distribution of potential.

This conductor is partially cut over a distance a, which represents the crack, as shown in Fig. 5. For a first approximation, if we assume that $L \gg b$, we may assume that the shaded zone is not crossed by the current. The cross-section is then reduced to $(L - a)e$. The resistance is thus:

$$R = \frac{\varrho b}{e(L - a)} \tag{2}$$

On substituting for R_0, as defined above, we obtain

$$\frac{a}{L} = 1 - \frac{R_0}{R} \tag{3}$$

This shows that there is a clear linear relation between the relative crack length and the relative conductance of the gauge. This is not usually the case for potentiometric techniques where the current is usually punctually fed, contrary to our hypothesis.

2.1. Distribution of potential

The electric potential was measured at different points on the conducting layer applied from a graphite spray ("Graphite 33", Kontakt Chemie, Rastatt, Germany) on a plate of PMMA. The surface of the graphite, of dimensions 250 mm by 10 mm, was bounded by two layers of silver paint (Leitsilber 200", Demetron, Hanau, Germany), and cut to simulate a crack as shown in Fig. 6.

These tests showed that the zone adjacent to the crack does indeed contribute to the overall conductance, contrary to our hypothesis above. The conductivity measured is given in Fig. 7 as a function of crack length. There is a linear region which deviates by a value Δ from the theoretical line. The principal consequence of these border effects is that the gauge has reduced accuracy at low values of initial crack length.

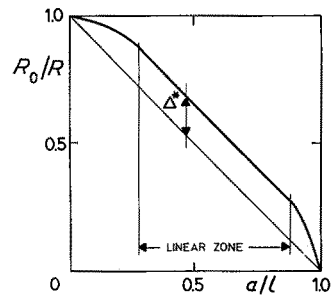

Figure 7 Relative conductivity of the gauge as a function of the relative crack length.

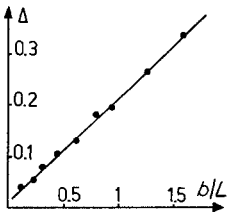

Figure 8 Deviation of the conductance due to the crack as a function of the relative width of the gauge.

The deviation Δ and the region in which the relationship between R_0/R and a/L is linear is governed by the dimensions of the gauge. The relationship between Δ and the relative dimensions of the gauge is shown in Fig. 8. This indicates that over the linear region the following equation is valid

$$\frac{R_0}{R} = 1 - \frac{a}{L} + \Delta \qquad (4)$$

where $\Delta \approx 0.2(b/L)$. The region of validity of this expression was determined experimentally by conductance measurements on graphite paper of various shapes and sizes. The deviation Δ increases with the relative width of the gauge, b/L, and thus for wide gauges the accurate working length is rather short (see Fig. 9); i.e. for cracks of length less than $0.4b$ and greater than $0.9L$, the gauge cannot be used with accuracy. These limitations do not pose a practical problem because in most fracture mechanics specimens the pre-crack length will be longer than this length of minimum detection of the gauge. Furthermore, the upper limit in the region of $0.9L$ is not normally of primary interest. Nevertheless it is extremely important to take this phenomenon in consideration and fabricate gauges as narrow as possible with respect to their width.

2.2. Fabrication of the gauge

In Section 1.1 the method of measurement of crack length by adhesive bonded gauges was criticized because of their lack of precision. If the mechanical properties are not adapted, the crack will not propagate simultaneously in the gauge and in the material under test. This difference becomes clear on testing a ductile material: the support of the gauge, which is normally an epoxy or phenolic resin, will only support small deformations and will therefore break when only the material under test deforms. In this case the crack length is overestimated. For precise

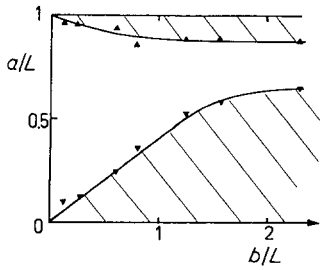

Figure 9 The measurable crack lengths are limited by the non-linear characteristic due to the presence of the crack. The measurement zone is defined as that region where the accuracy is better than $\pm 1\%$.

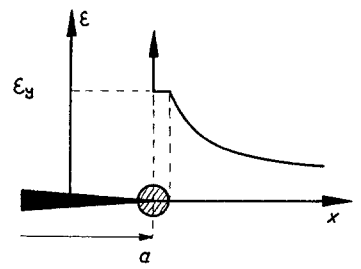

Figure 10 Deformation in the plane of the crack.

measurements the gauge must be able to support the deformation of the substrate without breaking. This appears rather restrictive at first sight. Considering the condition shown in Fig. 10, the local deformation in the axis of the crack tends to infinity for $x < a$. The point of singularity at $x = a$ marks the point of transition. If the deformation at break of the layer which constitutes the gauge is greater than ε_y, then the true crack length is measured. Two experimental systems fulfill this requirement: a thin layer of a very ductile metal; a layer of conducting particles of small size, not bound to each other but having sufficient adhesion to the specimen to follow its deformation. The second solution is much easier to apply. There are commercially available mixtures of graphite particles in a solvent with a polymeric binder which are sold in the form of an aerosol. These are sold for other purposes but are suitable for the majority of applications. It is, however, wise to conduct some preliminary experiments as the organic liquids which these sprays contain may induce the formation of crazes in certain polymers, or even be solvents for some materials. In other cases an inadequate surface tension may prevent a good wetting of the surface. The experimental worker must, in these cases, produce a suitable composition which can be applied by means of a reuseable aerosol. In cases where the surface is not grooved it is also possible to apply the gauge using the technique of silk screen printing. A homogeneous distribution of current is then obtained by applying two lines of conducting silver paint from a drawing pen, this paint is readily available in a colloidal solution and is frequently used for electron microscopy. According to the exact type of product the resistance varies between 0.01 and $0.03\,\Omega$, per unit surface area. This value is sufficiently low to obtain the desired effect. The drying time is less than 1 h at room temperature.

The conductivity as a function of the weight of graphite applied, is shown in Fig. 11. It can be seen

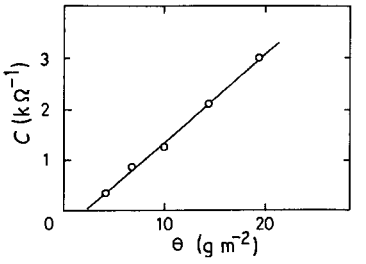

Figure 11 Conductivity of the gauge as a function of the amount of graphite applied.

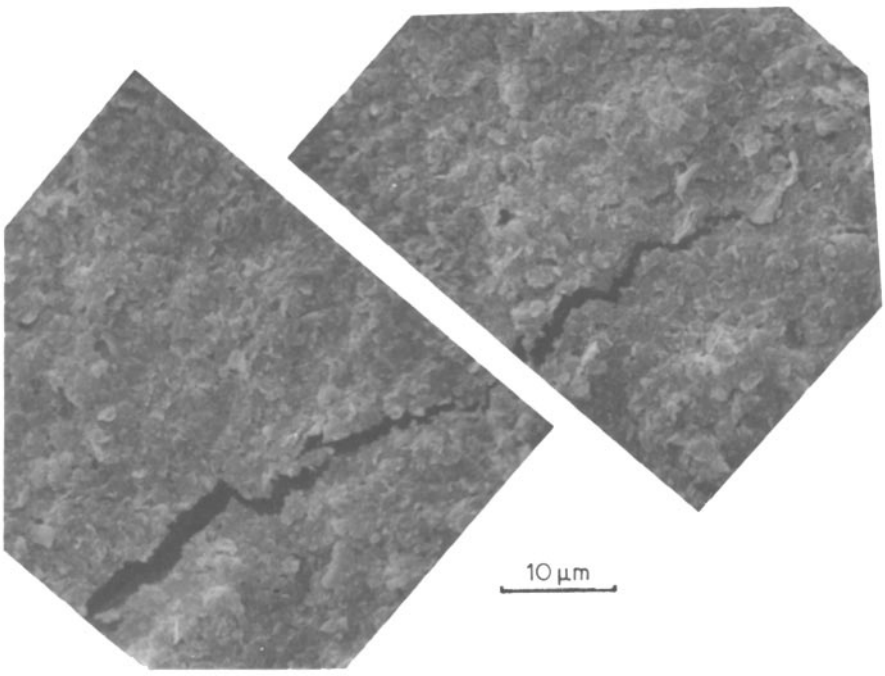

Figure 12 Scanning electron micrograph of the graphite layer around the crack tip.

that for the product used the conductivity is zero at less than 2 g graphite per square metre. Below this value the solution forms isolated particles of size characteristic of the aerosol used and the wetting of the surface. In order for the layer to retain its ability to follow accurately the deformation of the substrate, it must be thin but not so thin that discontinuities exist in the layer. These limitations restrict the layer to $\approx 10\,g\,m^{-2}$, that is thicknesses between 5 and 10 μm.

A typical graphite layer on a poly(aminobismaleimide) substrate, as viewed under the scanning electron microscope, is shown in Fig. 12. The structure of the graphite layer can be clearly seen together with the supposed point of the crack. Some bridges across the crack are also evident but their resistance is extremely high and only influences very slightly the overall conductivity. It can be seen from this figure that the opening displacement of the graphite, some 0.5 μm corresponds very well with the value, d, that can be calculated for this material from

$$d = \frac{K_c^2}{E\sigma_y} \qquad (5)$$

where $K_c = 0.5\,MPa\,m^{1/2}$, $\sigma_y = 120\,MPa$ is the yield stress $E = 2.8\,GPa$, then $d = 0.7\,\mu m$.

In spite of the extremely small crack opening displacement, d, in this material, the gauge appears to follow correctly the behaviour of the material. When this particular polymer is saturated with water it exhibits a stick–slip type of crack propagation which leaves clear marks on the fracture surface. This behaviour was used to correlate these fractographic marking with the values given by the graphite gauge. Fig. 13 shows crack propagation of this material in the double torsion geometry, a good correspondence is found between the two methods of determination of crack position.

2.3. Homogeneity of the layer

An aerosol spray is difficult to use when a large area must be covered with a constant thickness. According to the regularity of the spraying, variable results can be obtained which can significantly modify the measured conductance. A gauge of dimensions 280 mm × 80 mm can give rise to variations in potential which can vary by ±4% from the ideal distribution for a homogeneous layer of constant thickness (see Fig. 14). In this case the silk screen technique should be used for fabrication of the gauge. In our experience the spraying method is not applicable to lengths in excess of 100 mm.

2.4. Parallelism of the electrodes

If we ignore the other possible sources of error, it is possible to treat in a simple manner the condition where the two silver lines are not perfectly parallel (see

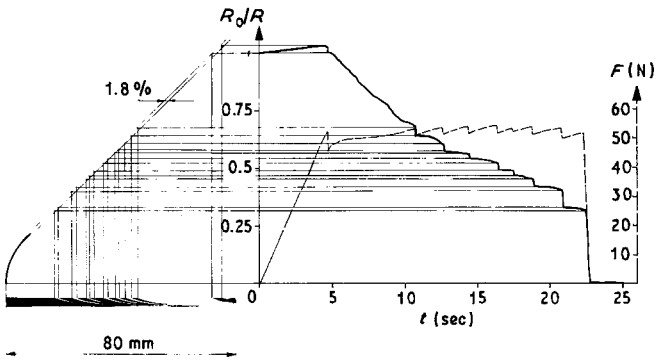

Figure 13 Fracture of a double torsion specimen showing the correlation between the output from the graphite gauge and the crack arrest lines observed on the fracture surface.

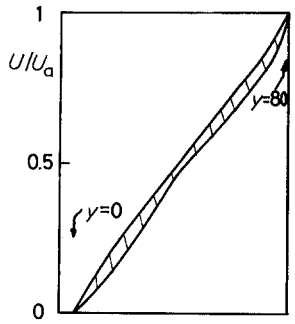

Figure 14 Distribution of potential in a gauge of size 280 mm × 80 mm (shaded area).

Fig. 15). Assuming that $\Delta = 0$, then the resistance of the gauge with a pre-crack of length a is

$$R = \rho \frac{b \pm (\Delta b/2) \pm (a/L)\Delta b}{(L - a)e} \quad (6)$$

The initial resistance is given by

$$R_0 = \rho \frac{L}{e} \quad (7)$$

The relative conductance can then be deduced

$$\frac{R_0}{R} = \left(1 - \frac{a}{L}\right)p \quad (8)$$

where

$$\frac{1}{p} = 1 \pm \frac{\Delta b}{b}\left(\frac{a}{L} + \frac{1}{2}\right) \quad (9)$$

The measurement of the crack length is defined by Equation 8. By comparing the measured value, a_m, and the real value, a, the following expression is obtained

$$\frac{a_m}{L} = 1 - \frac{R_0}{R} \quad (10)$$

and

$$\frac{a}{L} = 1 - \frac{1}{p}\frac{R_0}{R} \quad (11)$$

$$\frac{\Delta a}{a} = \frac{a_m - a}{a} = \frac{\Delta b}{b}\left(\frac{1}{2} - \frac{a}{L}\Big/1 + \frac{R_0}{R}\right) \quad (12)$$

The limiting conditions are clearly established: firstly that, $0 < a/L < 1$, and $0 < R_0/R < 1$ and secondly, that the error in a is no greater than one-half the error in b. If we allow an error of 1% in the measurement of a, the electrodes on a three-point bend specimen (where $L = 12.5$ mm) must be parallel to within 0.1 mm. It is clear that only very careful preparation of the gauge will ensure such accuracy.

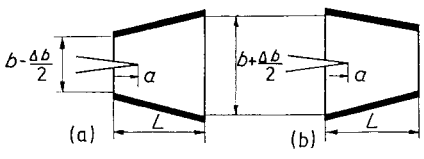

Figure 15 Gauges where the silver electrodes are not parallel.

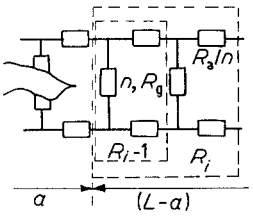

Figure 16 Modelling of a gauge as discrete elements.

2.5. Resistance of the silver electrodes

The choice of the conducting ink forming the two electrodes at the limits of the gauge, must be based on the resistivity of the layer obtained because the global resistance will depend on this factor.

If the gauge is divided into n slices which represent discrete elements (see Fig. 16), it is possible to estimate the influence of the resistance of the silver electrode (R_a) in comparison with the resistance of the graphite gauge (R_g) having a length of L and crack length $a = 0$. By a summation of the following equation between $i = 1$ and $i = n$, $(L - a)/L$

$$R_i = \left[\frac{1}{R_{i-1}} + \frac{1}{nR_g}\right]^{-1} + 2\frac{R_a}{n} \quad (13)$$

Fig. 17 shows the values obtained for four different ratios between the resistance of the graphite and that of the silver electrodes. The variation is linear and approximately equal to

$$\frac{\Delta a/a}{R_a/R_g} \approx 0.22 \quad (14)$$

A ratio $R_a/R_g = 0.05$ which would give an error of $\approx 1\%$ represents the least favourable experimental conditions. These would be for a gauge of length 100 mm, with $R_g = 200\,\Omega$ and $R_a = 10\,\Omega$. It is very easy to minimize the source of error by enlarging the width of the silver layer which thus reduces the value of R_a to less than $1\,\Omega$.

2.6. Overall accuracy of the gauge

The overall accuracy of the gauge was measured firstly by simulation of crack propagation. Gauges 80 mm

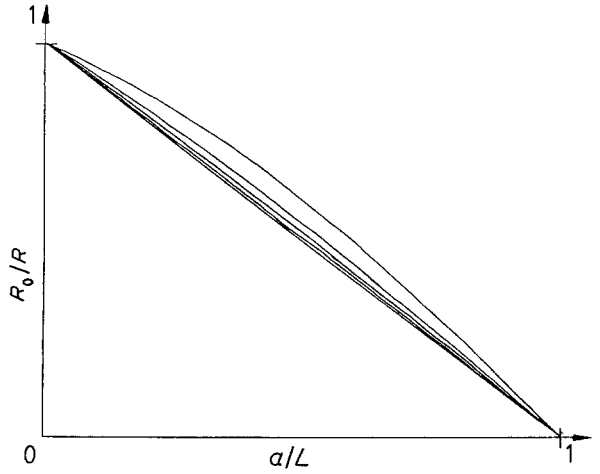

Figure 17 Relationship between relative crack resistance and relative crack length as a function of the relationship between the resistance of the electrode and that of the gauge. The number of elements, as shown in Fig. 16, was 100. $R_a/R_g = 0.05, 0.1, 0.2, 0.5$.

TABLE II The three principal sources of error in the measurement of crack length by the graphite gauge with assessment of their relative importance

Sources of error in decreasing order of importance	Notes
1. Strain Sensitivity	This should be checked with low modulus or tough materials and for specimen geometries where the loading is primarily tensile.
2. Measurement of the Current	With the voltage drop method, the choice of a very low shunt resistance helps to limit this error to under 1%. The disadvantage is the low values of voltage to be measured.
3. Parallelism of the electrodes	Careful fabrication enables the error to be limited, there are no other ways of overcoming this error.
4. Homogeneity of the layer	This becomes important for gauges of length > 100 mm produced by the spray method, below this limit the error is small. For longer gauges a different fabrication method should be selected to overcome this problem.
5. Resistance of the electrodes	This error can be eliminated by increasing the thickness and the width of the electrodes.

long were prepared and progressively cut by a rotating tool moving at a constant speed with respect to the specimen. The relationship between the conductivity and time was found to be linear to 1% of the total length of the gauge.

Secondly, the graphite gauges were compared with direct, optical measurements on compact tension, single-edge notch and double torsion specimens. In spite of the effect of the deformation of the gauge which is superimposed on the crack growth (see Section 2.7), the tests on these specimens validated the precision of the measurement.

The absolute accuracy of the gauge is typically of the order of ± 0.5 mm. The sensitivity is considerably better, it depends on the background noise, that is the instantaneous fluctuations of the resistance which is less than 0.1%. The worst case is at the beginning of the test when the crack is small and the resistance low

$$\frac{da}{a} \alpha \left[\frac{R(a)}{R_0}\right]^{-1} \tag{15}$$

It is thus possible to measure crack growth of 0.1 mm in a gauge 100 mm long. The sensitivity increases proportionally with the length for a shorter gauge. These measurements are based on an estimation of the errors derived from the three sources described above. A summary is given in Table II.

2.7. Sensitivity of the gauge to deformation

Deformation of a conducting material normally changes its electrical resistance. In the case of metals, the resistivity, r, varies due to the distortion of the crystalline lattice. In the case where the layer consists of particles, the resistivity can vary due to their relative displacement.

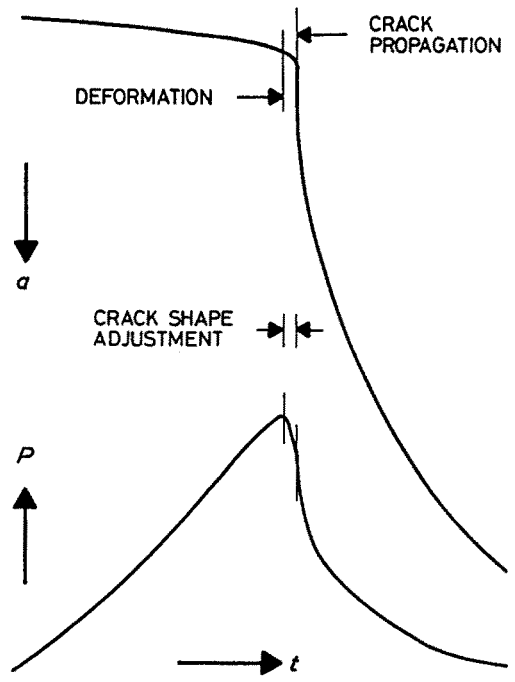

Figure 18 Output from the graphite gauge and the corresponding force–time diagram.

With most of the fracture mechanics geometries (except double torsion) a variable deformation is imposed perpendicular to the electrodes. The resistance must, therefore tend to increase as the specimen is loaded. This can be seen in Fig. 18.

In order to determine the sensitivity of the graphite gauge to deformation, a sheet of PMMA was prepared with a gauge having the electrodes parallel to the tensile axis. The deformation is ε_y and the lateral contraction $\nu\varepsilon_y$ (see Fig. 19). It is assumed that the graphite rigorously follows the behaviour of the polymer. Electron micrographs of the graphite layer (Fig. 12) suggest that the structure consists of superimposed flat discs. The thickness of the layer is thus most probably not modified.

The gauge factor, r, is defined as the ratio of the relative variation of the resistance and length with respect to the tensile direction

$$r = \frac{(\Delta\rho/\rho_0)}{\varepsilon_y} \tag{16}$$

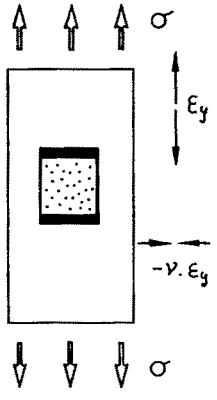

Figure 19 Test to show the sensitivity of the gauge to deformation. Under a stress, s, the deformations are respectively, ε_y and $-\nu\varepsilon_y$ in the two axes.

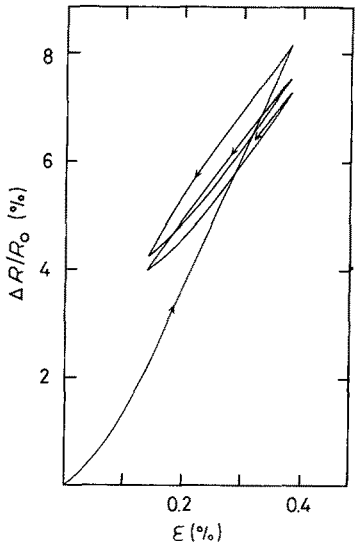

Figure 20 Reduction in the resistivity of the graphite after mechanical cycling of the load.

Gauge factors of the order of 20 were measured on samples of PMMA. The resistance of the graphite varies considerably due to the effective loss of surface contact between neighbouring particles. This state is not stable, cyclic deformations induce a continuous reduction in the resistivity (see Fig. 20). However, this does tend to stabilize after a large number of cycles. This significant hysteresis and the non-linearity of the curve means that it is not possible to define precisely a gauge factor. It would probably be illusionary to try and quantify elastic deformation with such a gauge and such a requirement it would be contradictory to the measurement of crack length.

The results do mean that certain geometries, such as single-edge notch, where the deformation is principally tensile, will be inherently more prone to this effect rather than geometries, such as compact tension or three-point bending, where the deformation occurs primarily in bending.

Strong biaxial deformation produced by plastic deformation drastically modifies the local conductivity. A notched bar of PVC tested at low speed in three-point bending, gave the curve shown in Fig. 21. The crack length given by the graphite gauge has been compared with photographs taken on the surface of the specimens (dimensions 50 mm × 12.5 mm × 10 mm). The plastic zone is clearly visible by its concave form. The limit of the plastic zone corresponds precisely to the measurements given by the gauge. In the zone of plastic deformation, the conductivity is less than one-tenth the original value. This is not so different to the result produced by a crack. For very ductile polymers, with large plastic zones, a continuous reduction in resistance will be observed as a function of deflection. This means that it is not always possible to distinguish between the first crack growth. In many cases, however, with experience the point of inflection of the curve can be detected. In the case of brittle polymers, such as thermosetting resins, the plastic zone is frequently 100 μm or less and therefore this problem does not arise.

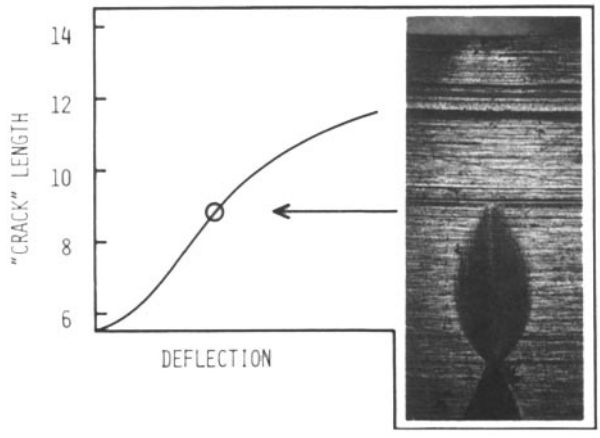

Figure 21 Comparison of optical and electrical measurement of crack advance.

2.8. Environmental effects

The rearrangement of the graphite particles is not only produced by deformation but also by the effect of temperature. At a temperature of 100° C, this decrease in resistance is stabilized in less than 1 h. This factor should be taken into account if the gauge is used at elevated temperatures.

The presence of high humidity or solvent vapour also increases the resistance of the gauge, probably due to the loss of contact between adjacent particle on which the molecules have been adsorbed. Equilibrium must be attained prior to the test and maintained throughout.

2.9. Electrical characteristics

The particulate nature of the gauge implies that the real current density at the contact points between particles is variable and several times higher than the apparent current density. This is given by $j = U/(\rho b)$, where U is the output voltage. The percolation effect limits the maximum intensity of current that may be used. It was confirmed that a current of 0.01 A mm^{-1} can be applied to a gauge for several hours without any appreciable variation in the measured resistance. In these conditions the heat produced by the Joule effect is partially dissipated into the atmosphere. The surplus induces a temperature rise on the surface of a few degrees centigrade. If the applied voltage is increased notably then the glass transition temperature of the support material could be attained. In any case, as shown in Fig. 22, the current–voltage relationship is no longer linear above 6 V. This should then be the maximum applied voltage.

A preliminary test conducted under the chosen experimental conditions (U, b, L, T, t, etc.) will verify whether the resistance remains constant and whether the sample temperature does not rise significantly, etc. Tests at high speeds also indicated that possible capacitative effects are low and do not interfere with fast crack propagation.

3. Experimental arrangement

3.1. Power supply

The graphite gauge is powered by a d.c. voltage supply set at a voltage between 2 and 6 V, typically a 5 V supply is used to ensure the required long-term stability.

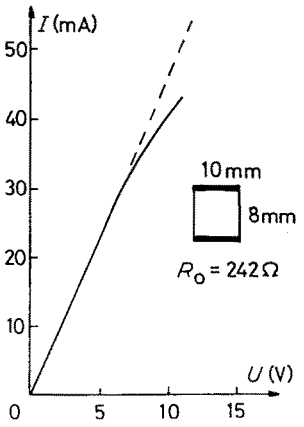

Figure 22 Relationship between current and voltage for a gauge of standard quality. The relationship is no longer linear for a supply voltage greater than 6 V.

3.2. Measurement circuit

Two ways have been used successfully to measure the voltage drop across the gauge. One solution is to drive the current passing through the gauge into a current-to-voltage converter which consists of an operational amplifier with a feedback resistor. The output voltage, U_m, depends on the input current, I_{in}, and the feedback resistor, R_f

$$U_m = I_{in} R_f \tag{17}$$

As I_n is a function of the gauge resistor, R_x, and the supply voltage, V_0

$$I_n = \frac{V_0}{R_x} \tag{18}$$

and then

$$U_m \approx U_0 \frac{R_f}{R_x} \tag{19}$$

with

$$R_x = \frac{R_0}{1 - (a/L)} \tag{20}$$

$$\frac{U_m}{U_0} = \frac{R_f}{R_0}\left(1 - \frac{a}{L}\right) \tag{21}$$

A second solution consists of placing a wirewound potentiometer R_v in series with the graphite gauge. The resulting current is then equal to $U_0/(R_x + R_v)$. A value of R_v of less than 10 Ω was chosen as this is sufficiently small compared with an R_0 of 300 to 1000 Ω. The voltage drop in R_v may be approximated by $U_m \approx U_0(R_v/R_x)$. The relationship between conductance and crack length becomes

$$\frac{U_m}{U_0} = \frac{R_v}{R_0}\left(1 - \frac{a}{L}\right) \tag{22}$$

The current-to-voltage circuit results in a lower error of measurement than the shunt method. However, the advantage of the second method is that in high-speed crack propagation the response time of the shunt is faster than that of the feedback amplifier due to its purely resistive behaviour. The shunt method has always been employed to measure high crack velocities: speeds of up to 900 m sec^{-1} have been recorded.

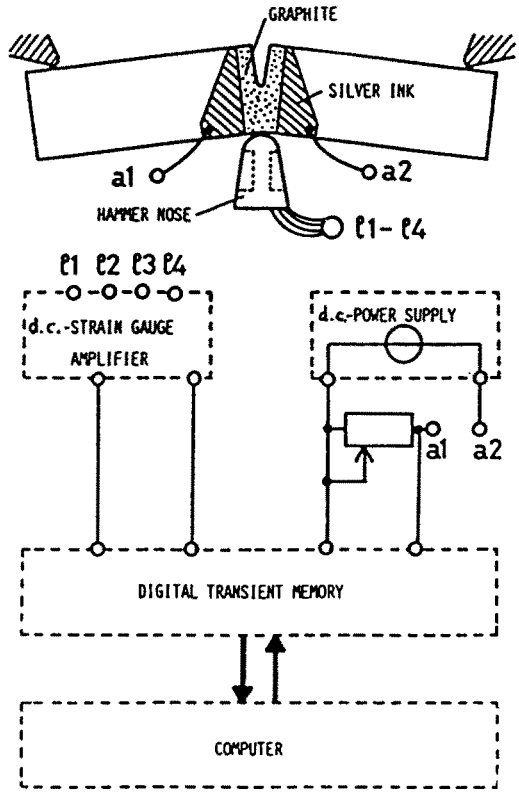

Figure 23 Experimental arrangement for the graphite gauge as applied to an impact specimen.

3.3. Example of application to a Charpy impact test

An example of the experimental arrangement as applied to a Charpy impact test is shown in Fig. 23. The strain gauge circuit on the instrumented striker is powered by a stabilized power supply and connected via an amplifier to one channel of the digital transient recorder. The graphite gauge is powered by a separate power supply and connected via a resistive shunt to the second channel of the transient recorder. This recorder (WW Instruments) has a programmable trigger such that a certain proportion of the total memory may be chosen to be retained before the trigger. The trigger is set at, for example, 90% of the voltage output of the gauge; with storage of 25% of the total memory capacity before the trigger. In this manner a simultaneous recording of the load–crack length–time profile is obtained. The transient recorder has a standard interface which permits the transfer of the data on to a minicomputer.

4. Applications to the fracture testing of polymers

The objective of the publication is to describe the nature of the graphite gauge but not to give a large number of examples of its application to various systems. Existing publications have already cited some applications [25–30]. Nevertheless, three examples will serve as an illustration here.

4.1. Charpy impact test on a Polyamide 12

In Fig. 24 the crack length–time profile and the corresponding crack speed–crack length profile are shown for a Charpy test on a polyamide 12. Under the

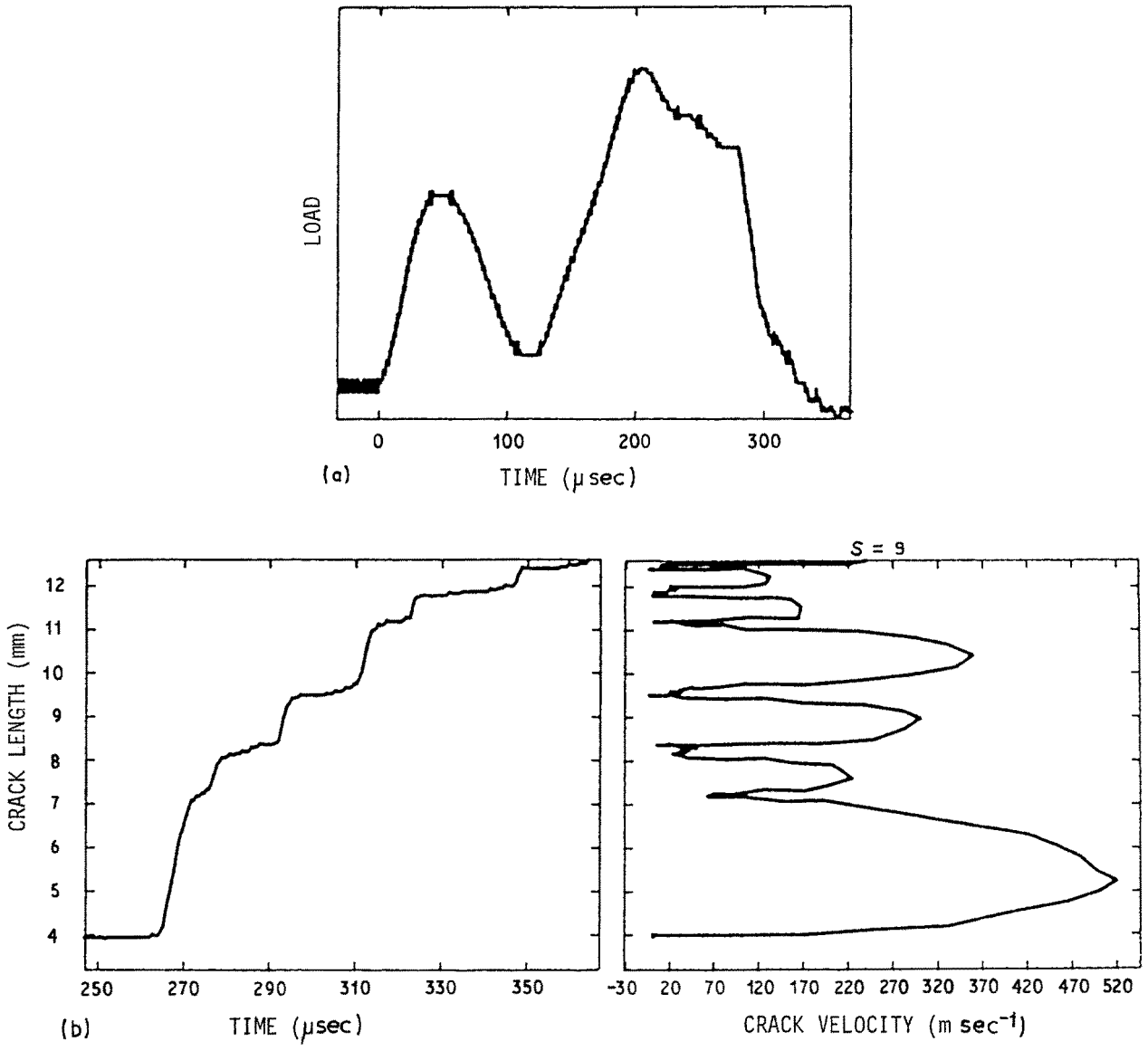

Figure 24 Output of the graphite gauge and corresponding force–time diagram for a Polyamide 12 sample (Charpy test).

conditions of this test the crack accelerates very rapidly up to 500 m sec^{-1} and thereafter a number of jumps are recorded where the crack slows down. The corresponding load–time profile shows a complex pattern of oscillation of the load on the striker which is supposed to be due to the contact and loss of contact between the striker, the specimen and the supports [26]. The interpretation of these load oscillations is still rather difficult. The output from the graphite gauge, however, gives valuable information on the exact time at which a crack initiates. This can be correlated with the load at the same point in time if account is taken of the differing response times of the two electrical circuits. Furthermore, the data on the maximum crack velocity attained and the crack speeds during jumps in "stick–slip" propagation can give valuable insight into the mechanisms of crack propagation in polymers [31].

4.2. Relationship between fracture surface morphology and crack velocity

The graphite gauge has proved to be very useful for the correlation of certain features on the fracture surface and the crack speed. Tests on silica-filled epoxy resins showed clearly that the fracture morphology changed over the range of speeds measured which was from 10^{-6} to 10^{2} m sec^{-1}. By a combination of tensile creep tests and fracture mechanics tests it was possible to characterize several regimes of crack velocity and their effect on the fractographic features. This work is described in detail by Cantwell *et al.* [29]. One example of the results is given in Fig. 25, which shows the fracture surface of a silica-filled epoxy resin tested in the single-edge notch tensile mode. It can be seen that the crack velocity accelerates rapidly up to a maximum speed of 850 m sec^{-1}. During the phase of acceleration the fracture surface is smooth as the excess stored elastic energy is used in increasing the crack speed. Once the maximum speed is reached it is no longer possible to accelerate the crack further and another energy dissipating mechanism must be found. Here, the energy is dissipated by crack bifurcation giving rise to a very rough three-dimensional surface for this filled material.

4.3. Crack propagation across the interface between two materials

The graphite gauge can also be applied to study crack propagation across interfaces [32]. An example is given in Fig. 26 where a single-edge notch sample

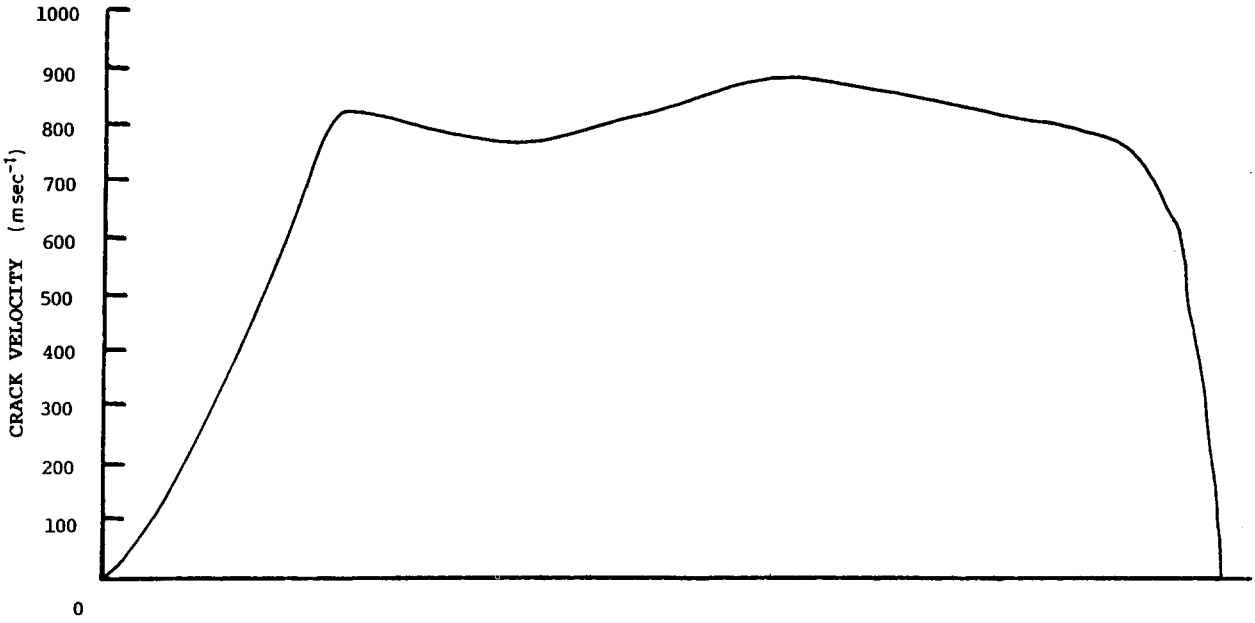

Figure 25 The variation of crack velocity across the surface of a single-edge notch specimen – silica-filled epoxy resin (from [30]).

has been prepared with two phases, A and B. In the corresponding crack length–time profile it can be seen that rapid crack propagation occurs in material A, followed by crack arrest for a period of 800 μsec. Finally, there is initiation of a crack in material B followed by slower crack propagation. The graphite gauge can give useful information on the criteria for crack deceleration or arrest at the interface between dissimilar materials.

5. Conclusions

The performance of the graphite gauge is tightly linked to the type of polymer being tested. Although the original idea was to measure the crack velocity in highly cross-linked and consequently brittle polymers, the results presented show that the usefulness of this method is not restricted to this application. We may summarize the advantages and disadvantages of the graphite gauge as follows.

5.1. Advantages

1. Applicable for crack speed measurement over a wide range of temperatures.
2. Sensitivity of crack position down to 0.1 mm.
3. Wide range of crack speeds can be measured from 10^{-7} to 10^{3} m sec^{-1}.
4. Values can be readily digitalized for subsequent storage of data and analysis.
5. Technique is cheap and can be applied to a large number of samples.

5.2. Disadvantages

1. The measurement is only as good as the quality of the graphite layer and the electrodes, thus great care must be exercised in fabrication of the gauge.
2. For ductile materials having a large plastic zone it may not be possible to distinguish between crack growth and the development of the plastic zone at the crack tip.

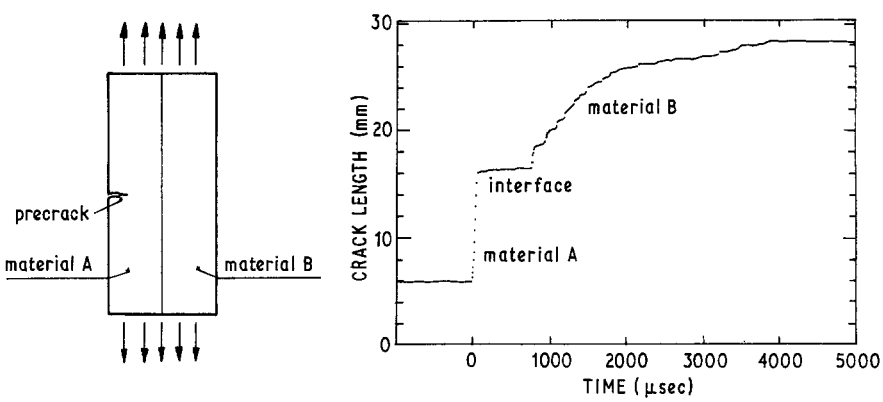

Figure 26 Two-phase single-edge notch specimen and crack length–time profile during a tension test.

References

1. A. S. KOBAYASHI, "Experimental Techniques in Fracture Mechanics", Vols 1 and 2 (Iowa State University Press, Ames, Iowa, and Society for Experimental Stress Analysis, Wesport, Connecticut, 1975).
2. C. J. BEEVERS (ed.), "Advances in Crack Length Measurement" (Chamelon, London, 1982).
3. K. F. STARK, J. DENK and G. KIESLING, *Mater. Technik* **2** (1983) 43.
4. F. KERKHOF, "Fracture des verres" (Saint-Gobain Industries, 1974).
5. T. A. MICHALSKE and V. D. FRÊCHETTE, *Int. J. Fract.* **17** (1981) 251.
6. W. F. DEANS and C. E. RICHARDS, 5th International Conference on Fracture (ICF5) Cannes, April 1981, p. 1989.
7. *Idem, J. Test. Eval.* **7** (1979) 147.
8. C. E. RICHARDS and W. F. DEANS, in "The measurement of Crack Length and Shape during Fracture and Fatigue", edited by C. J. Beevers (EMAS, West Midlands, UK) p. 28.
9. G. A. D. BRIGGS, N. A. FLECK and R. A. SMITH, "Advances in Crack Length Measurement", edited by C. J. Beevers (Chamelon, London, 1982) p. 395.
10. A. R. BLYTHE, "Electrical Properties of Polymers" (Cambridge University Press, 1979).
11. S. K. BHATTACHARYA and A. C. D. CHAKLADER, *Polym.-Plast. Technol. Engng* **19** (1982) 21.
12. *Idem, Ibid.* **20** (1983) 35.
13. J. M. LOWES and G. D. FEARNEHOUGH, *Engng Fract. Mech.* **3** (1971) 103.
14. G. CLARK and J. F. KNOTT, *J. Mech. Phys. Solids* **23** (1975) 265.
15. R. O. RITCHIE and K. J. BATHE, *Int. J. Fract.* **15** (1979) 47.
16. F. D. W. CHARLESWORTH and W. D. DOVER, in "Advances in Crack Length Measurement", edited by C. J. Beevers (Chamelon, London, 1982) p. 253.
17. G. BAUDIN and H. POLICELLA, 5th International Conference on Fracture (ICF5) Cannes, April, 1981, p. 1957.
18. P. C. PARIS and B. R. HAYDEN, ASTM Symposium on Fatigue Crack Growth, Pittsburgh, October 1979 (American Society for Testing and Materials, Philadelphia, Pennsylvania).
19. M. J. GUEURY and R. V. DIEUDONNE, *NDT Int.* June (1979) 121.
20. A. KOBAYASHI and N. OHTANI, *J. Appl. Polym. Sci.* **24** (1979) 2255.
21. A. KOBAYASHI, N. OHTANI and M. MUNEMURA, *ibid.* **25** (1980) 2789.
22. Y. M. MAI and P. R. KERR, *J. Mater. Sci. Lett.* **23** (1984) 971.
23. G. A. BRIGGS, in "Advances in Crack Length Measurement", edited by C. J. Beevers (Chamelon, London, 1982) p. 447.
24. O. BUCK and B. R. TITTMANN, *J. Mater. Sci.* **20** (1985) 413.
25. M. T. RESCH, D. V. NELSON and J. C. SHYNE, in "Advances in Crack Length Measurement", edited by C. J. Beevers (Chamelon, London, 1982) p. 473.
26. B. STALDER, PhD thesis, Ecole Polytechnique Fédérale de Lausanne, no. 586 (1985).
27. B. STALDER and H. H. KAUSCH, *J. Mater. Sci.* **20** (1985) 2481.
28. H. R. BEER, T. KAISER, A. C. MOLONEY and H. H. KAUSCH, *ibid.* **21** (1986) 3661.
29. W. J. CANTWELL and A. C. ROULIN-MOLONEY, *Int. J. Fract.* **35** (1987) R39.
30. W. J. CANTWELL, A. C. ROULIN-MOLONEY and T. KAISER, *J. Mater. Sci.* **23** (1988) 1615.
31. W. J. CANTWELL, A. C. ROULIN-MOLONEY and H. H. KAUSCH, *J. Mater. Sci. Lett.* **7** (1988) 976.
32. A. C. ROULIN-MOLONEY, unpublished work, 1987.

Received 7 April
and accepted 5 September 1988